Properties and structure of *a*-SiC:H for high-efficiency *a*-Si solar cell

Y. Tawada,[a] K. Tsuge,[a] M. Kondo, H. Okamoto, and Y. Hamakawa
Faculty of Engineering Science, Osaka University, Machikaneyamacho 1-1, Toyonaka, Osaka 560, Japan

(Received 4 January 1982; accepted for publication 12 February 1982)

A series of experimental investigations on optical and optoelectronic properties of methane- and ethylene-based *a*-SiC:H films has been made. The chemical bonding structure of two kinds of *a*-SiC:H films has also been explored from infrared (IR) absorption structural analysis. An experimental verification for the wide gap window material in the amorphous silicon solar cell is shown on methane- and ethylene-based *a*-SiC:H. The methane-based *a*-SiC:H film shows one or two orders of magnitude larger photoconductivity recovery effect of doping than the ethylene-based one. IR absorption analysis shows that the methane-based *a*-SiC:H film is recognized as a rather ideal amorphous SiC alloy as compared with the ethylene-based one. It has been found through these investigations that the methane-based *a*-SiC:H film is superior to the ethylene-based one as a window material. Utilizing the methane-based *a*-SiC:H, an 8% efficiency barrier has been broken through with an *a*-SiC:H/*a*-Si:H heterojunction structure.

PACS numbers: 84.60.Jt

I. INTRODUCTION

A hydrogenated amorphous silicon carbide was first reported by Anderson and Spear.[1] Since their work, IR[2–4] and photoluminescence[5,6] analysis, and a study in the plasma reaction mechanism[7] of undoped *a*-SiC:H, have been given. However, any information on the effect of impurity doping on the basic properties of *a*-SiC:H has not been reported. Meanwhile, we have made efforts to control the valency electrons of wide gap materials for the purpose of improving the efficiency of *p-i-n a*-Si solar cells. Recently, a good valency electron controllability has been found in a hydrogenated amorphous silicon carbide prepared by the plasma decomposition of an $[SiH_{4(1-x)} + CH_{4(x)}]$ gas mixture.[8,9]

An *a*-SiC:H film can be fabricated by the decomposition of silane (SiH_4) and hydrocarbon gas mixture,[1,7] or alkylsilane.[10] However, the structural and optoelectronic properties of *a*-SiC:H films might be significantly dependent upon both carbon sources and deposition conditions. Utilizing ethylene (C_2H_4) and methane (CH_4) as carbon sources, we have fabricated *a*-SiC:H films and have conducted a series of experimental investigations of the optoelectronic properties in these materials. We have also examined the relationship between the structural, optical, and electrical properties of these films.

It has been found through these investigations that the methane-based *a*-SiC:H is almost constructed with tetrahedrally coordinated carbons or carbons attached with a hydrogen, and is superior to the ethylene-based *a*-SiC:H for a window material in a *p-i-n a*-Si solar cell. In this paper, a series of optical and optoelectronic properties, and IR spectra of *a*-SiC:H films prepared by the decomposition of the $[SiH_{4(1-x)} + CH_{4(x)}]$ or $[SiH_{4(1-x)} + \frac{1}{2}C_2H_{4(x)}]$ gas mixture, are demonstrated and discussed with a view toward adding insight into the structural basis. The photovoltaic performances of *a*-SiC:H/*a*-Si:H heterojunction solar cells are also discussed.

[a] On leave of absence from Kanegafuchi Chemical Industry Co. Ltd., 1-2-80 Yoshida-cho, Hyogo, Kobe 652, Japan.

II. EXPERIMENTAL DETAILS

a-SiC:H films were prepared in the plasma deposition system as described in our previous paper[11–13] by the decomposition of $[SiH_{4(1-x)} + CH_{4(x)}]$ or $[SiH_{4(1-x)} + \frac{1}{2}C_2H_{4(x)}]$. Both Corning No. 7059 glass and high-resistive single-crystal silicon wafers were used as substrates. They were subjected to standard cleaning techniques and then N_2-plasma-bombardment treatment for ten minutes prior to the onset of deposition. The substrate temperature was held at 250 °C; the rf power was kept at 35 W, and the total gas flow fixed at 100 sccm. The used gas, SiH_4, CH_4, C_2H_4, B_2H_6, and PH_3 were diluted with H_2. The thicknesses of deposited films were 5000 Å for optical and optoelectronic measurements, and 10 000 Å for IR measurements. IR spectra were measured by a double-beam Fourier-transfer IR spectrometer (FT-IR, Digilab. FTC-15c) to obtain high resolution. The blank silicon substrate was set in the reference beam.

III. PHOTOCONDUCTIVITY AND OPTICAL BAND GAP OF UNDOPED AND BORON-DOPED *a*-SiC:H FILMS

The optical band gap of *a*-SiC:H films was determined from the straight-line intercept of a $(\alpha h\omega)^{-1/2}$-vs-$h\omega$ curve in the high-absorption region ($\alpha > 10^4$ cm^{-1}) following the analysis of Davis and Mott.[14] It seems unreasonable to measure the photoconductivity of *a*-SiC:H films having optical band gaps ranging from 1.76 to 2.2 eV under the same monochromatic illumination. Therefore, we measured AM-1 photoconductivity (100 mW/cm^2) and also monochromatic photoconductivity under the illumination light of the wavelength at which the *a*-SiC:H film has the same optical absorption coefficient ($\alpha = 10^4$ cm^{-1}). The monochromatic photoconductivity was normalized to the $\eta\mu\tau$ product proposed by Zanzucchi *et al.*[15] Comparing this $\eta\mu\tau$ product with AM-1 photoconductivity among various compositional *a*-SiC:H films, an obvious positive correlation has been found among them.[9] From these results it is recognized that AM-1 photoconductivity can be used as a convenient characterization tool for the optoelectronic properties of *a*-SiC:H films.

 0021-8979/82/075273-09$02.40

Figure 1 shows the AM-1 photoconductivity σ_{ph} and the optical band gap $E_{g(opt)}$ of undoped and boron-doped *a*-SiC:H films prepared by the decomposition of $[SiH_{4(1-x)} + CH_{4(x)}]$. AM-1 photoconductivity of undoped *a*-SiC:H films significantly decreases with increasing methane fraction. On the other hand, boron-doped films show 1 or 3 orders of magnitude larger photoconductivity as compared with undoped films. These photoconductivity recovery effects have been similarly seen in phosphorous-doped *a*-SiC:H films. These effects are accompanied by the decrease of electron spin resonance (ESR) spin density by doping. In other words, boron or phosphorus atoms would compensate the dangling bond in the amorphous SiC network, and thus enhance the carrier lifetime.

The optical band gap of undoped and boron-doped *a*-SiC:H increases monotonically with increasing methane fraction, but $E_{g(opt)}$ of boron-doped films is a little bit narrower than undoped films. This narrowing of $E_{g(opt)}$ by doping is mainly caused by the decrease of hydrogen content attached to the carbon.

Figure 2 shows the optical band gap $E_{g(opt)}$ and AM-1 photoconductivity σ_{ph} of undoped and boron-doped *a*-SiC:H films prepared by an $[SiH_{4(1-x)} + \frac{1}{2}C_2H_{4(x)}]$ gas mixture. The optical band gap of these ethylene-based *a*-SiC:H films increases from 1.76 to 2.8 eV with increasing ethylene fraction. The reason why the ethylene-based *a*-SiC:H film shows a larger optical band gap in the same gas-phase carbon fraction is that the carbon content in the ethylene-based *a*-SiC:H film is larger than that of the methane-based *a*-SiC:H

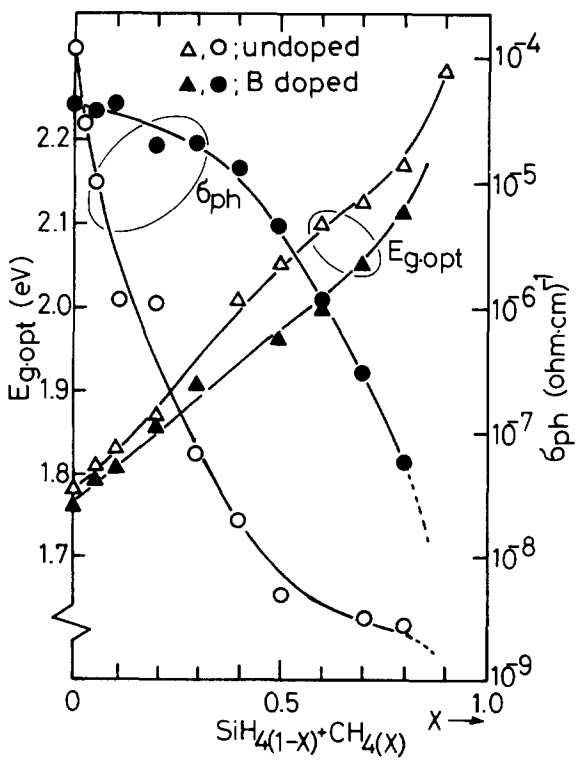

FIG. 1. Photoconductivity σ_{ph} and optical band gap $E_{g(opt)}$ of undoped and boron-doped *a*-SiC:H films prepared by the decomposition of $[SiH_{4(1-x)} + CH_{4(x)}]$ gas mixture.

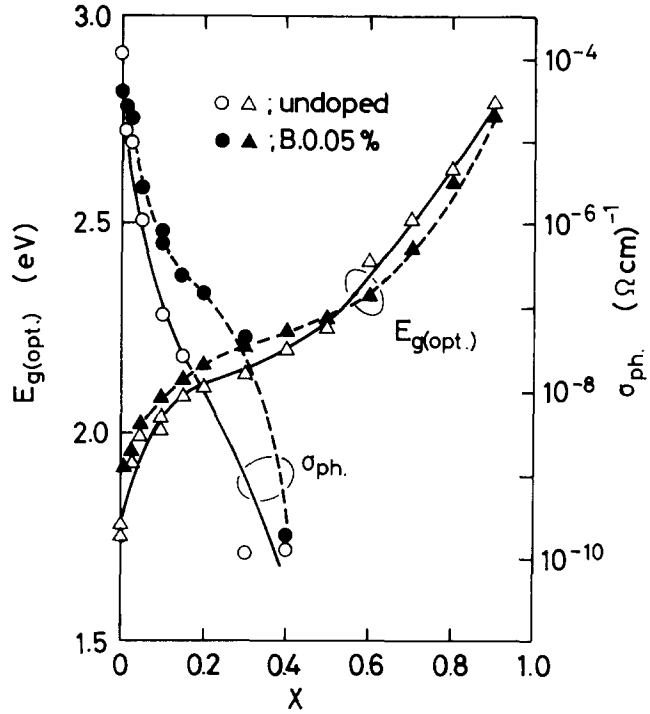

FIG. 2. Photoconductivity σ_{ph} and optical band gap $E_{g(opt)}$ of undoped and boron-doped *a*-SiC:H films prepared by the decomposition of $[SiH_{4(1-x)} + \frac{1}{2}C_2H_{4(x)}]$ gas mixture.

film. It is interesting in this case that $E_{g(opt)}$ of boron-doped *a*-SiC:H films is larger in the gas fraction by less than 0.5, and smaller in the gas fraction by more than 0.5, than that of undoped *a*-SiC:H films. The hydrogen content attached to silicon (Si) is not affected by boron doping but the hydrogen content attached to carbon (C) is affected by boron doping; that is, these narrowing and widening effects are caused by the hydrogen attached to carbon.

In the range where the optical band gap widening occurs, the photoconductivity of boron-doped *a*-SiC:H based on ethylene is only one order of magnitude larger than that of undoped *a*-SiC:H. Comparing the ethylene-based *a*-SiC:H and the methane-based *a*-SiC:H, it is recognized that the methane-based *a*-SiC:H shows one or two orders of magnitude larger photoconductivity recovery effect of boron doping than the ethylene-based *a*-SiC:H. The amount of hydrogen atoms attached to carbon is a factor responsible for this photoconductivity recovery effect.

IV. IR SPECTRA ANALYSIS AND STRUCTURE OF *a*-SiC:H

Methane-based *a*-SiC:H films show 1 or 2 orders of magnitude larger photoconductivity recovery effect of boron doping than ethylene-based *a*-SiC:H films. To understand the difference between the two, the chemical bonding structure of the methane-based and the ethylene-based *a*-SiC:H has been investigated by means of IR spectra. Figure 3 shows the typical IR spectra of boron-doped *a*-SiC:H films. The carbon content of these films might be estimated to be about 12 at.% for Auger electron spectroscopy (AES peak ratio C/Si = 0.06, and crystalline SiC standard). *a*-SiC:H films exhibit four main absorption regions. The absorption

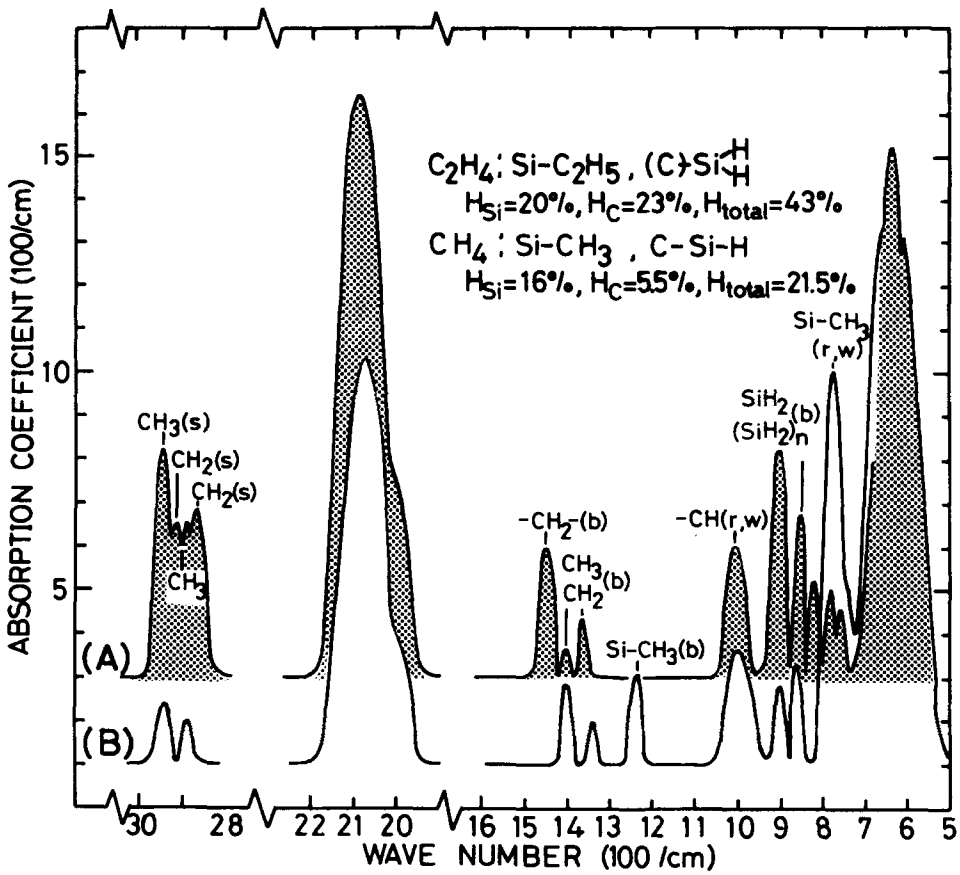

FIG. 3. Infrared spectra of a boron-doped ethylene-based *a*-SiC:H film (*A*) and a boron-doped methane-based *a*-SiC:H film (*B*).

band between 2800 and 3000 cm^{-1} is the C-H stretching mode. This absorption band is so weak that each fine peak has not yet been exactly assigned.[4] There are four distinct peaks in the ethylene-based *a*-SiC:H: 2940, 2910, 2890, and 2870 cm^{-1}. On the other hand, the methane-based *a*-SiC:H film shows only two peaks: 2940 and 2890 cm^{-1}. The 2940-cm^{-1} peak was assigned to the CH_3 stretching by Wieder *et al.*[2] The 2940- and 2890-cm^{-1} peaks can be attributed to CH_3 stretching because the 1450-cm^{-1} band absorption which could be identified as a $-CH_2-$bond is seen in the ethylene-based *a*-SiC:H film but not in the methane-based one. Meanwhile, the CH stretching absorption is very weak, in general; therefore, the 2910- and 2850-cm^{-1} peaks which are observed in ethylene-based *a*-SiC:H might also be assigned to CH_2 stretching.

The absorption band between 1500 and 1200 cm^{-1} is the CH_n bending mode. The 1450-cm^{-1} peak which is observed only in the ethylene-based *a*-SiC:H has not yet been assigned. Owing to the analogy from alkylsilane derivatives,[16] the 1450-cm^{-1} peak could be identified as the $-CH_2-$ bending mode. Another typical peak is 1250-cm^{-1}, which is due to the symmetric bending mode of the CH_3 attached to silicon.[2] This peak can be seen only in the methane-based *a*-SiC:H film. It is recognized through these investigations that the ethylene-based *a*-SiC:H film does not contain the Si-CH_3 bonds.

The strongest feature in these spectra also occurs at 780 cm^{-1}. This peak was assigned to the Si-CH_3 rocking or wagging mode by Wieder *et al.*[2] However, Katayama *et al.*[17] concluded that this peak was assigned to the Si-C stretching mode, because this peak could be seen in the sputtered *a*-SiC without hydrogen. In our experiment, the 780-cm^{-1} peak absorption is four times stronger in the methane-based *a*-SiC:H film ($\alpha = 900$ cm^{-1}) than in the ethylene-based *a*-SiC:H film ($\alpha = 210$ cm^{-1}). If one can assume 780 cm^{-1} to be attributed to Si-CH_3, this result is consistent with the 1250-cm^{-1} peak.

From the facts described above, we may conclude that carbons are almost incorporated as ethyl (C_2H_5) group in the ethylene-based *a*-SiC:H, and are incorporated as a methyl (CH_3) group in the methane-based *a*-SiC:H. However, carbon content as a Si-CH_3 bond in the methane-based *a*-SiC:H is only 1 or 2%.

Another strong feature in these spectra can be seen in the 860–890-cm^{-1} band which is assigned to the SiH_2 or $(SiH_2)_n$ bending mode by Brodsky[18] and Fritzsche.[19] In amorphous silicon films deposited in the same chamber in the absence of carbon sources, this band is too weak to detect. Meanwhile, this absorption band can be seen in *a*-SiC:H films, especially in ethylene-based *a*-SiC:H films. This result shows that carbons promote silicon dihydride bonds in amorphous networks. The 890-cm^{-1} peak absorption coefficient of the methane-based and the ethylene-based *a*-SiC:H films are 350 and 1100 cm^{-1}, respectively, so that the ethylene-based *a*-SiC:H film contains about a three times larger content of silicon dihydride than the methane-based *a*-SiC:H films. Corresponding to this result, the 2000–2100-cm^{-1} band is larger in the ethylene-based *a*-SiC:H film than in the methane-based *a*-SiC:H film. The 2090- and 2000-cm^{-1} peaks of *a*-SiC:H film was assigned to the SiH_2 and SiH

stretching modes.[18,19] It is well known that the 2000-cm^{-1} peak shifts toward a higher wave number region by the presence of carbon attached to silicon.[2] This shift can be related to the electronegativity of the carbon substituent.[20] Using the relation obtained by Lucovsky,[20] the SiH and SiH_2 stretching frequency in *a*-SiC:H films can thus be represented as

$$\nu_{SiH}\ (cm^{-1}) = 1740.7 + 34.7 \sum_{i=1}^{3} X(R_i) \pm 13,$$

and

$$\nu_{SiH_2}\ (cm^{-1}) = 1956.3 + 25.4 \sum_{i=1}^{2} X(R_i) \pm 12.$$

From these equations one can estimate the influence of neighboring atoms on the frequency of SiH and SiH_2 attached to one, two, and three carbon atoms. The results are summarized in Table I. The 2090-cm^{-1} peak is inferred to any of the SiH_2 stretching modes, and the SiH mode attached with one or two carbons to silicon. Considering that the carbon content of these films is rather small (AES peak ratio C/Si = 0.06), it might be possible that the 2090-cm^{-1} peak is assigned to the stretching mode absorption of SiH attached with one carbon to silicon.

a-SiC:H films deposited at room temperature show the 2120-cm^{-1} peak which might be due to the stretching absorption of SiH_2 attached with one carbon atom to silicon. From the result of the SiH_2 bending mode absorption, it is assumed that the 2090-cm^{-1} peak in the ethylene-based *a*-SiC:H film is contained in a larger amount of the SiH_2 bond ($\nu_{SiH_2} = 2090\ cm^{-1}$ and $\nu_{c\text{-}SiH_2} = 2120\ cm^{-1}$) than in the methane-based *a*-SiC:H film.

The hydrogen content of *a*-SiC:H films was evaluated with the following expressions (Ref. 18):

$$N_H = A_s \int_{\nu_s} \frac{\alpha(\nu)}{\nu}\, d\nu,$$

where

$$A_s = \begin{cases} 1.4\times10^{20}\ (cm^{-1}) & \text{for } SiH_n \text{ (Ref. 21)} \\ 1\times10^{21}\ (cm^{-1}) & \text{for } CH_n \text{ (Ref. 3)} \end{cases}.$$

The results are summarized in Fig. 3. The content of hydrogen attached to Si is 20 and 16 at. % for the ethylene-based and the methane-based *a*-SiC:H, respectively. The content of hydrogen attached to C is 23 and 5.5 at. % for the ethylene-based and the methane-based *a*-SiC:H films, respectively. The most important feature can be seen in the carbon-attached hydrogen which is a four times larger amount in the ethylene-based *a*-SiC:H film than in the methane-based film. Assuming that carbons are incorporated as a C_2H_5 group in the ethylene-based *a*-SiC:H and as a CH_3 group in the methane-based film, one can estimate the amount of Si–C_2H_5 and Si–CH_3 bond: 9.2 at.% carbons are incorporated as a –C_2H_5 group in the ethylene-based *a*-SiC:H film and 1.8 at.% carbons are incorporated as a –CH_3 group in the methane-based *a*-SiC:H film. Other carbons (about 10%) are incorporated as terahedrally bonded carbons or carbons attached with one hydrogen (C–H) in the methane-based *a*-SiC:H.

TABLE I. Calculated stretching frequency of Si–H bond.

Monohydride (Si–H)		Dihydride ($Si–H_2$)	
39MSi Si–Si–H Si	2013 cm^{-1}	Si Si–H_2 Si	2092 cm^{-1}
Si C–Si–H Si	2054 cm^{-1}	C Si–H_2 Si	2119 cm^{-1}
C C–Si–H C	2095 cm^{-1}	C Si–H_2 C	2149 cm^{-1}
C C–Si–H C	2135 cm^{-1}		

It is recognized from these investigations that the methane-based *a*-SiC:H is a rather ideal amorphous SiC alloy in contrast to the ethylene-based *a*-SiC:H, which is an organosilane-like structure. It might be basically caused by the structural differences between the two; the methane-based *a*-SiC:H film shows 1 or 2 orders of magnitude larger photoconductivity recovery effect of doping than the ethylene-based film. Furthermore, this structural difference affects the photovoltaic performances of *a*-SiC:H/*a*-Si:H heterojunction solar cells. The results are discussed in Sec. V.

V. EFFECT OF METHANE-BASED AND ETHYLENE-BASED *a*-SiC:H ON PHOTOVOLTAIC PERFORMANCES

The structure and the optoelectronic properties of glow-discharge-produced *a*-SiC:H films are strongly dependent upon the carbon sources, as is discussed in Secs. III and IV. To confirm a wide gap window effect of *a*-SiC:H we have fabricated *a*-SiC:H/*a*-Si:H heterojunction solar cells. The cell structure is glass/SnO_2/*p a*-SiC:H/*i*-*n a*-Si:H/Al. The substrate temperature is about 250 °C, and the layer thicknesses of *p a*-SiC:H, undoped *a*-Si:H, and *n a*-Si:H films are 100, 5000, and 500 Å, respectively. The deposition conditions of undoped and phosphorous-doped ($Ph_3/SiH_4 = 0.5\%$) *a*-Si:H were described in our previous report.[13] The activation energy of the *p* layer in the *p*-*i*-*n a*-Si solar cells is generally required to be less than 0.6 eV, and the conductivity of the *p* layer in these same solar cells is more than $10^{-7}\ (\Omega\ cm)^{-1}$. Therefore, the *p*-type methane-based and the ethylene-based *a*-SiC:H films having band gaps ranging from 1.8 to 2.2 eV were adopted, whose activation energy and conductivity were settled about 0.55 eV, and on the order of $10^{-7}\ (\Omega\ cm)^{-1}$, respectively. The sensitive area of solar cells is 3.3 mm^2, which was carefully evaluated to be about 5% larger than the aluminum-deposited bottom electrode (3.14 mm^2) by taking into account the experimentally confirmed edge effects to photocurrent.[8] *J*-*V* characteristic measurements were carried out under AM-1 solar illumination (100 mA/cm^2).

Figure 4 shows the photovoltaic performances of *a*-SiC:H/*a*-Si:H heterojunction solar cells as a function of the optical band gap $E_{g\,(opt)}$ of *p*-type methane-based *a*-SiC:H film. As is seen in this figure, the short circuit current density J_{sc} and the open circuit voltage V_{oc} increase as the size of the optical band gap of *p* layer increases. A required factor to

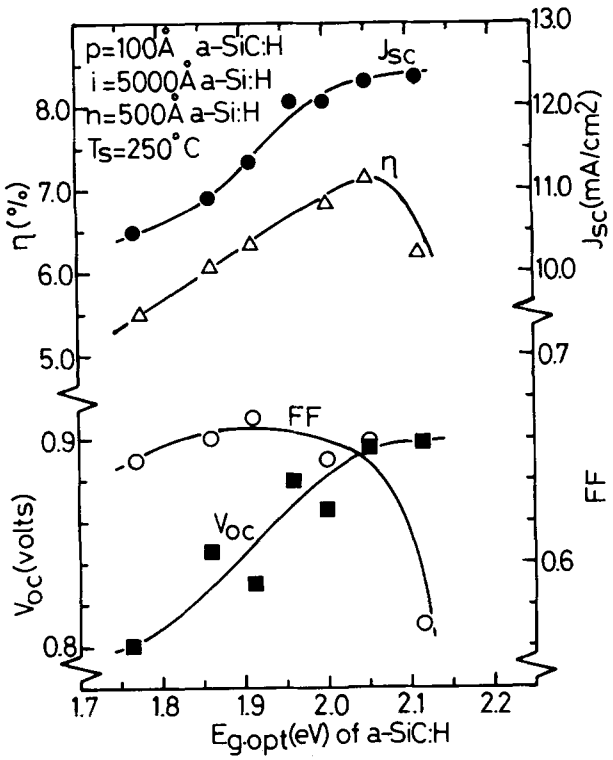

FIG. 4. Photovoltaic performances of methane-based a-SiC:H/a-Si:H heterojunction solar cells as a function of the optical band gap $E_{g(opt)}$ of p-type methane-based a-SiC:H.

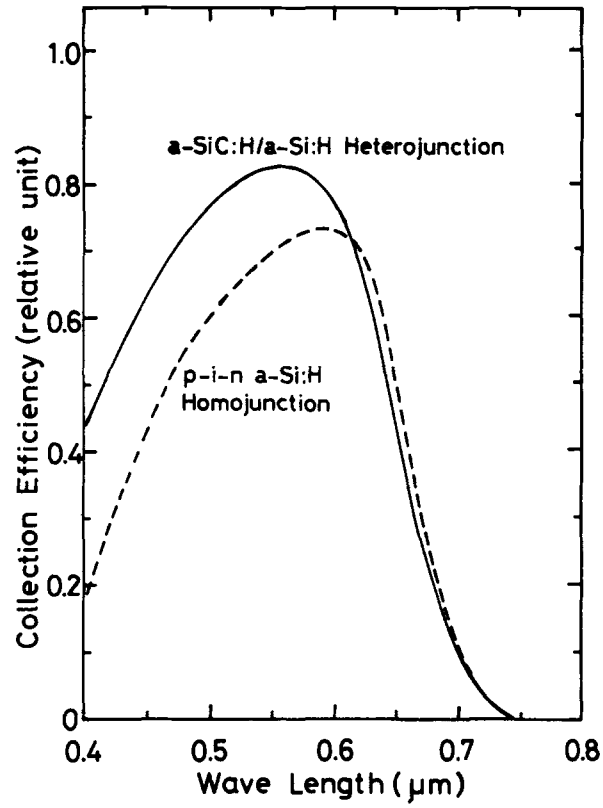

FIG. 5. Collection efficiency of an ordinary p-i-n a-Si:H homojunction solar cell and a typical a-SiC:H/a-Si:H heterojunction solar cell.

increase the short circuit current density is to effectively introduce the incident photons into the i layer, where the photocurrent is mainly produced.[22] The increase of J_{sc} is first due to the wide gap window of a-SiC:H. Another effect of the increased band gap in the p layer is a corresponding increase in the blocking barrier for electrons at the p-i interface. The alignment of conduction band in the a-SiC:H/a-Si:H heterojunction structure was chosen so that the discontinuity appears in the band edge at the p-i interface. Therefore, the back diffusion of electrons from the i into the p layer might be practically blocked. This blocking barrier effect is remarkable, especially in the short-wavelength region of incident photons. The experimental evidence can be seen in the collection efficiency spectra. Figure 5 shows the collection efficiency data of an ordinary p-i-n a-Si:H homojunction solar cell and an a-SiC:H/a-Si:H heterojunction solar cell. The collection efficiency of this heterojunction solar cell is improved by more than two times at the short-wavelength region as compared with the homojunction solar cell, while this improvement is only 20% at a wavelength of 550 nm. It is concluded that the increase of collection efficiency at the short-wavelength region is caused mainly by the blocking barrier in the p-i interface of the a-SiC:H/a-Si:H heterojunction solar cell.

The increase of the open circuit voltage is also caused by a wide gap window effect due to the potential profile steepened with a wide gap a-SiC:H. This point will be discussed further in this article.

Figure 6 shows the photovoltaic performances of a-SiC:H/a-Si:H heterojunction solar cells as a function of the optical band gap $E_{g(opt)}$ of ethylene-based a-SiC:H. In spite of the optical band gap increase of the p layer, the short circuit current density J_{sc} of these cells is smaller in the range 1.9–2.13 eV than that of the p-i-n a-Si:H homojunction solar cell ($E_{g(opt)} = 1.76$ eV). In the ethylene-based a-SiC:H/a-Si:H heterojunction cell, it seems that a energy spike exists at the p-i interface in the valence band edge. Because holes cannot traverse freely into the p layer, the photocurrent might be limited in the ethylene-based a-SiC:H/a-Si:H heterostructure.

The distinction of the photocurrent between the methane- and ethylene-based a-SiC:H/a-Si:H heterojunction solar cell may be due to the structural difference as discussed above. It is concluded that wide gap amorphous materials are not always useful as window side junction materials, and that the structure of these materials is an important factor for junction formation.

As for the voltage factor of a-SiC:H/a-Si:H heterojunction solar cells, we found a clear correlation between the open circuit voltage V_{oc} and the diffusion potential V_d in the methane-based a-SiC:H/a-Si:H heterojunction solar cells.[13,23] In the ethylene-based a-SiC:H/a-Si:H heterostructure, the open circuit voltage increases as the optical band gap of the ethylene-based a-SiC:H increases. The same correlation can also be seen in this case, as shown in Fig. 7. The diffusion potential V_d can be changed by controlling the doping fraction and the rf power in the deposition of the p layer. The open circuit voltage of these cells is plotted on the same correlation between V_{oc} and V_d. The chemical bonding structure of a-SiC:H depends upon a carbon source, doping fraction, and preparation condition. Therefore, the voltage

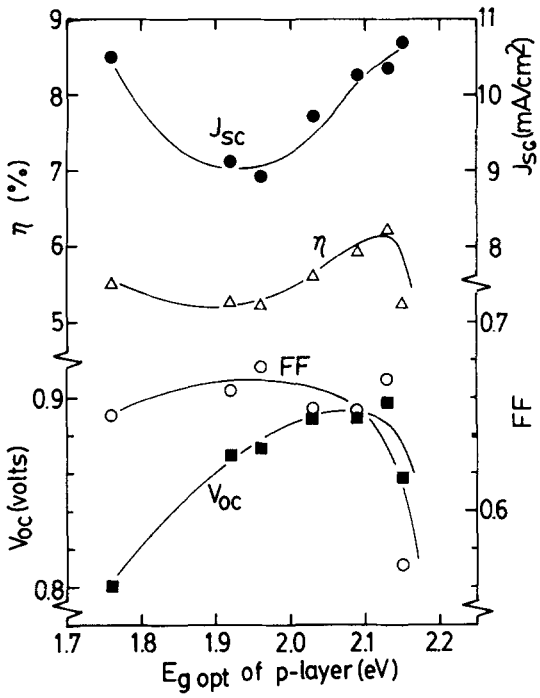

FIG. 6. Photovoltaic performances of ethylene-based a-SiC:H/a-Si:H heterojunction solar cells as a function of the optical band gap $E_{g(opt)}$ of p-type ethylene-based a-SiC:H.

factor might be independent of the structure of a-SiC:H, and the correlation between V_{oc} and V_d is consistent, in general. From this correlation, it is recognized experimentally that 1/3 of the increased diffusion potential contributes to the increase of the open circuit voltage of the solar cell.

VI. TYPICAL PHOTOVOLTAIC PERFORMANCES OF a-SiC:H/a-Si:H HETEROJUNCTION SOLAR CELLS

It has been found through these investigations that the methane-based a-SiC:H film is a rather ideal amorphous SiC alloy, and is superior to the ethylene-based one for the window material. Figure 8 shows the typical photovoltaic performances of the methane- and ethylene-based a-SiC:H/a-Si:H heterojunction solar cells which were obtained on the same substrate. The performances of the methane-based a-SiC:H/a-Si:H cell are $\eta = 7.82\%$, $J_{sc} = 13.76\,\text{mA/cm}^2$, $V_{oc} = 0.903$ V, and FF = 62.9%. On the other hand, the performances of the ethylene-based a-SiC:H/a-Si:H cell are $\eta = 6.21\%$, $J_{sc} = 10.34\ \text{mA/cm}^2$, $V_{oc} = 0.897$ V, and FF = 67.0%. As is seen in these data, the J_{sc} of the methane-based a-SiC:H/a-Si:H heterojunction cell is 33% larger than the J_{sc} of the ethylene-based cell.

Utilizing this methane-based a-SiC:H as a window side p layer, the performance of a-SiC:H/a-Si:H heterojunction solar cells has been improved. As a result, we have succeeded in breaking through an 8% efficiency barrier with this new material. Typical performances of the a-SiC:H/a-Si:H heterojunction solar cell are $J_{sc} = 15.2\ \text{mA/cm}^2$, $V_{oc} = 0.88$ V, FF = 60.1%, and $\eta = 8.04\%$ with a glass/antireflective ITO substrate, as shown in Fig. 9. The interface between the transparent electrode and the p layer is important to improve the efficiency of large-area solar cells.[24] We have developed a glass/ITO-SnO_2(100 Å) substrate to improve the interface. Employing this substrate, 7.7% efficiency of 1.0-cm² solar cell has been obtained, as shown in Fig. 10. The corresponding performances of this cell are $J_{sc} = 14.06\ \text{mA/cm}^2$, V_{oc}

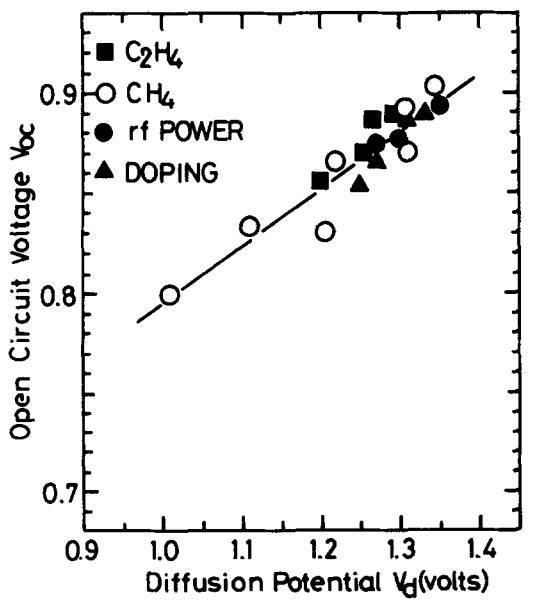

FIG. 7. Correlation between the open circuit voltage V_{oc} and the diffusion potential V_d of a-SiC:H/a-Si:H heterojunction solar cells as parameters of carbon sources, rf power of p layer deposition, and doping fraction of p layer.

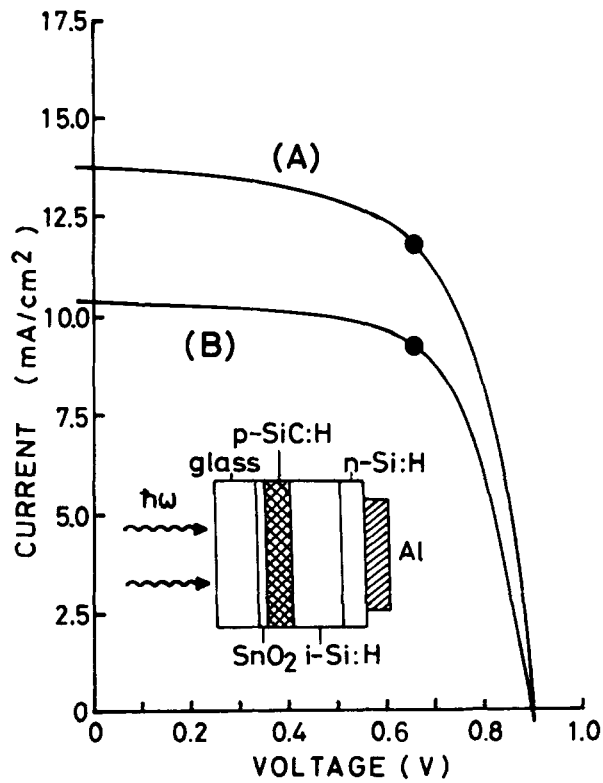

FIG. 8. J-V characteristics of a methane-based a-SiC:H/a-Si:H heterojunction solar cell (A) and an ethylene-based a-SiC:H/a-Si:H heterojunction solar cell (B) with the glass/SnO_2 substrate. Sensitive area = 3.3 mm², $P_{in} = 100\ \text{mW/cm}^2$. ($A$): $V_{oc} = 0.903$ V, $J_{sc} = 13.76\ \text{mA/cm}^2$, FF = 62.9%, and $\eta = 7.82\%$. (B): $V_{oc} = 0.897$ V, $J_{sc} = 10.34\ \text{mA/cm}^2$, FF = 67.0%, and $\eta = 6.21\%$.

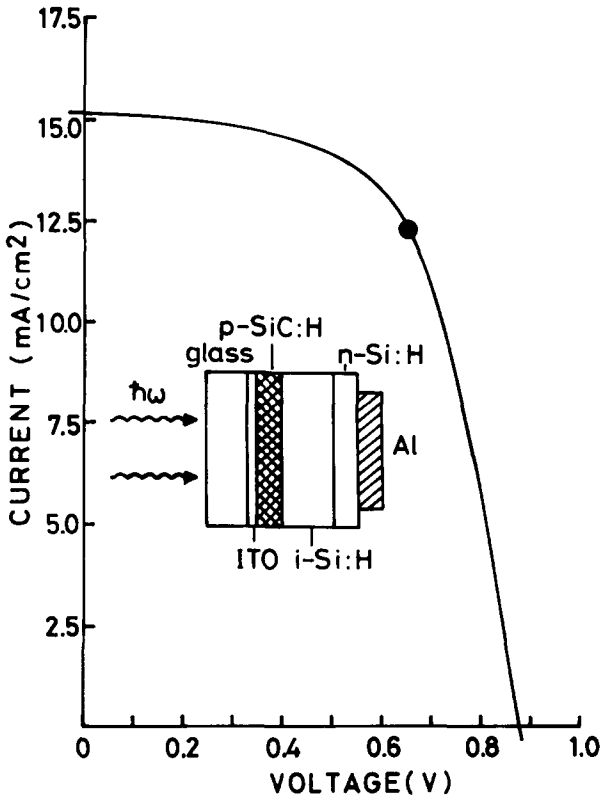

FIG. 9. J-V characteristics of 8% efficiency a-SiC:H/a-Si:H heterojunction solar cell with the glass/antireflective ITO substrate. Area = 3.3 mm^2, P_{in} = 100 mW/cm^2, V_{oc} = 0.880 V, J_{sc} = 15.21 mA/cm^2, FF = 60.1%, and η = 8.04%.

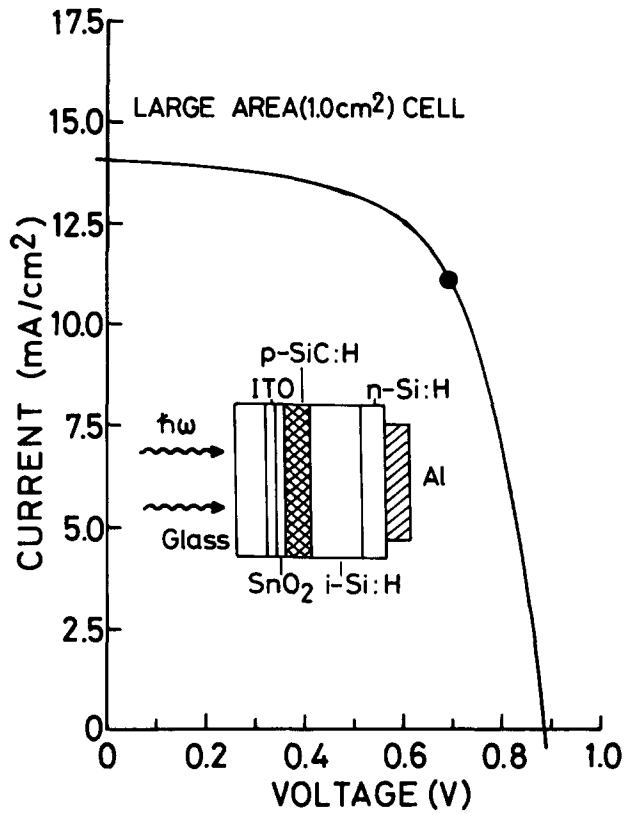

FIG. 10. J-V characteristics of a large-area a-SiC:H/a-Si:H heterojunction solar cell with the glass/ITO/SnO_2 substrate. Area = 1.0 cm^2, P_{in} = 100 mW/cm^2, V_{oc} = 0.880 V, J_{sc} = 14.06 mA/cm^2, FF = 62.4%, and η = 7.7%.

= 0.880 V, and FF = 62.4%. These results show that a-SiC:H is a very favorable window material.

VII. DISCUSSION AND SUMMARY

Amorphous SiC:H films which have a wide band gap can be fabricated by the plasma decomposition of silane and hydrocarbon gas mixture. However, the optoelectronic properties and the chemical structure of a-SiC:H films might be significantly dependent upon both carbon sources and deposition conditions. The optical band gap can be controlled in the range 1.8–2.2 eV by controlling the gas fraction of $[SiH_{4(1-x)} + CH_{4(x)}]$. The optical band gap can also be controlled in the range 1.8–2.8 eV by controlling the gas fraction of $[SiH_{4(1-x)} + \frac{1}{2}C_2H_{4(x)}]$. We have conducted a series of experimental studies of the optoelectronic properties in the methane- and ethylene-based a-SiC:H films. We have also examined the relationship between the chemical structure and the electrical and optical properties of these a-SiC:H films.

The photoconductivity of undoped a-SiC:H films sharply decreases with increasing carbon fraction. On the other hand, the methane-based a-SiC:H films show 1 or 3 orders of magnitude larger photoconductivity recovery effect of boron doping. In contrast with this, the ethylene-based a-SiC:H films show only 1 order of magnitude larger photoconductivity recovery effect of boron doping. The photoconductivity recovery effect has also been seen in a phosphorus-doped a-SiC:H film. It is recognized from ESR measurements that this effect is caused by the decrease of ESR spin density; boron and phosphorus atoms compensate the dangling bonds in the a-SiC:H network.

The boron doping on the methane-based a-SiC:H film gives rise to the narrowing of the optical band gap. On the other hand, the boron doping on the ethylene-based a-SiC:H film gives rise to the widening of the optical band gap in the carbon gas-phase fraction range less than 0.5, and to the narrowing of the optical band gap in the carbon gas-phase fraction greater than 0.5. These narrowing and widening effects of boron doping are caused mainly by the hydrogen attached to carbon.

To examine the origin of the optical and optoelectronic differences between the methane- and ethylene-based a-SiC:H films, the chemical structures of these a-SiC:H films have been investigated by means of IR spectra. It is recognized from the investigation of C–H stretching and bending mode absorption that the ethylene-based a-SiC:H film contains carbons as a $-C_2H_5$ group and the methane-based a-SiC:H film contains as a $-CH_3$ group. On the other hand, the content of hydrogen attached to Si can be estimated to be 20 and 16 at.% for the ethylene-based and the methane-based a-SiC:H films, respectively. The content of hydrogen attached to C can be estimated to be 23 and 5.5 at.% for the ethylene- and the methane-based a-SiC:H films, respectively. Assuming that carbons are incorporated as a $-C_2H_5$ group for the ethylene-based a-SiC:H film and as a $-CH_3$ group for the methane-based a-SiC:H film, we can estimate the Si–C_2H_5 bond and the Si–CH_3 bond: 9.2% carbons are incorporated as a $-C_2H_5$ group in the ethylene-based a-

SiC:H film, and 1.8% carbons are incorporated as a $-CH_3$ group in the methane-based *a*-SiC:H film. The carbon content of these films might be estimated to be about 12 at.% from the Auger Electron Spectroscopy (AES peak ratio C/Si = 0.06, and crystalline SiC standard). Therefore, carbon atoms are almost incorporated as a $-C_2H_5$ group in the ethylene-based *a*-SiC:H which has a large amount of SiH_2 bond. On the other hand, 1.8 at.% carbons are incorporated as a $-CH_3$ group and other carbons are incorporated as tetrahedrally bonded atoms in the methane-based *a*-SiC:H. It is recognized from these results that the methane-based *a*-SiC:H is a rather ideal amorphous SiC alloy in contrast to the ethylene-based *a*-SiC:H, which has an organosilane-like structure. It might be because of this structural difference that the methane-based *a*-SiC:H films show 1 or 2 orders of magnitude larger photoconductivity recovery effect of doping than the ethylene-based *a*-SiC:H films.

So as to confirm the wide gap window effect of these *a*-SiC:H films, we fabricated *a*-SiC:H/*a*-Si:H heterojunction solar cells. In the methane-based *a*-SiC:H/*a*-Si:H cell, not only the short circuit current density but also the open circuit voltage increases as the width of the optical band gap of the *p* layer increases. An essential factor required to increase the short circuit current density is to effectively introduce the incident photons into an *i* layer, where the photocurrent is mainly produced. The increase of J_{sc} is primarily due to the wide gap window of *a*-SiC:H. Another effect of *a*-SiC:H is a corresponding increase in the blocking barrier for electrons at the *p-i* interface. The alignment of the conduction band in the *a*-SiC:H/*a*-Si:H heterojunction structure was chosen so that the discontinuity appeared in the band edge at the *p-i* interface. Therefore, the back diffusion of electrons from the *i* layer to the *p* layer might be practically blocked. The experimental evidence can be seen in the collection efficiency, especially in the short-wavelength region. The collection efficiency of the methane-based *a*-SiC:H/*a*-Si:H cell is improved to be more than two times in the short-wavelength region as compared with that of an *a*-Si:H *p-i-n* homojunction cell, while this improvement is only 20% at the wavelength 0.55 μm.

On the other hand, the short circuit current density of the ethylene-based *a*-SiC:H/*a*-Si:H cell is smaller in the *p* layer optical band gap range 1.9–2.13 eV than the short circuit current density of the *a*-Si:H *p-i-n* homojunction cell, in spite of the wide gap *p* layer. In this case, it seems that the energy spike might exist at the *p-i* interface in the valence band edge, and holes cannot traverse freely into the *p* layer. The distinction of the short circuit current density between the ethylene-based and the methane-based *a*-SiC:H as a window material may be due to the difference of the chemical bonding structure between the two, as discussed above. It can be concluded that wide gap materials are not always useful as a window material for *p-i-n a*-Si solar cells, and that the chemical bonding structure of these materials is an important factor for junction formation.

Concerning the voltage factor of *a*-SiC:H/*a*-Si:H heterojunction solar cells, we have found a clear correlation between the open circuit voltage and the diffusion potential in both the methane- and ethylene-based *a*-SiC:H/*a*-Si:H heterojunction cells. The diffusion potential of these cells can be changed by controlling the doping fraction or the rf power in the deposition of the *p* layer. In this case, the correlation is consistent. Therefore, the voltage factor might be independent of the chemical bonding structure. It is recognized from this correlation that 1/3 of the increased diffusion potential contributes to the increase of open circuit voltage.

It has been found through these systematic investigations that the methane-based *a*-SiC:H film is a rather ideal amorphous SiC alloy, and is superior to the ethylene-based film as a window material. Utilizing this methane-based *a*-SiC:H, we have succeeded to break through an 8% efficiency barrier with *a*-SiC:H/*a*-Si:H heterojunction cells. Typical performances of this cell are $J_{sc} = 15.2$ mA/cm^2, $V_{oc} = 0.88$ V, FF = 60.1%, and $\eta = 8.04\%$ with the sensitive area of 3.3 mm^2. With a solar cell of larger area (1.0 cm^2), 7.7% efficiency has been obtained with $J_{sc} = 14.06$ mA/cm^2, $V_{oc} = 0.88$ V, and FF = 62.4%.

Furthermore, the top data of J_{sc}, V_{oc}, and FF separately obtained, as shown in Fig. 11, in *a*-SiC:H/*a*-Si:H heterojunction solar cells are 15.2 mA/cm^2, 0.91 V, and 71%, respectively. If we assume these realistic top data will become a typical routine performance on one cell, the efficiency of 9.8% might be obtained in the near future with this *a*-SiC:H/*a*-Si:H heterojunction solar cell.

ACKNOWLEDGMENTS

The authors wish to thank Professor A. Hiraki and Dr. T. Imura of Osaka University, and S. Kubo of Kanegafuchi

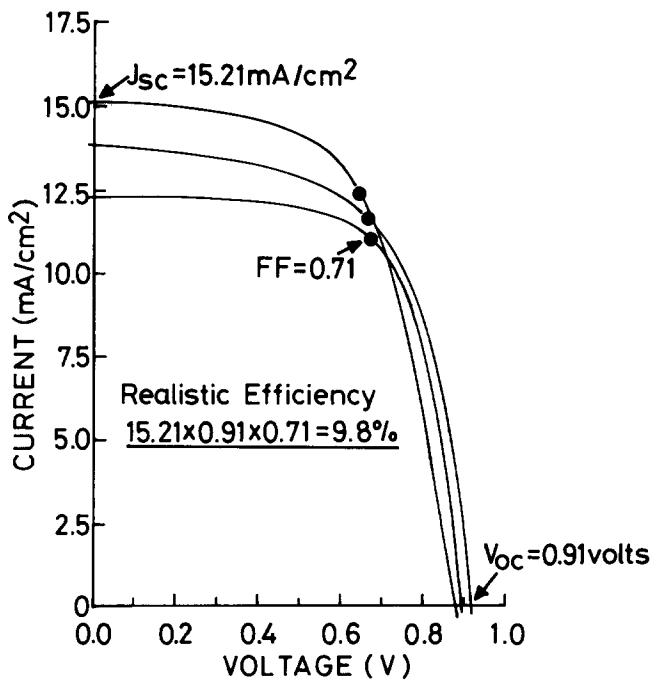

FIG. 11. Separately obtained top data of $V_{oc} = 0.91$ V, $J_{sc} = 15.2$ mA/cm^2, and FF = 71% on *a*-SiC:H/*a*-Si:H heterojunction solar cells, and the realistic efficiency (3.3 mm^2, $P_{in} = 100$ mW/cm^2), which will be obtained in the near future with this new solar cell.

Chemical Industry Co., Ltd., for helpful discussions. Technical assistance by C. Sada is acknowledged. The authors also thank K. Nishimura and K. Fujimoto for first response measurements. This work was partially supported by the Special Research Project on Amorphous Materials and Physics, sponsored by the Ministry of Education, Science, and Culture, and by the Sunshine Project Solar Photovoltaic Division, sponsored by the Agency of Industrial Science and Technology.

[1]D. A. Anderson and W. E. Spear, Philos. Mag. **35**, 1 (1977).
[2]H. Wieder, M. Cardona, and C. R. Guarnieri, Phys. Status Solidi B **92**, 99 (1979).
[3]A. Guivarch, J. Richard, M. LeContellec, E. Ligeon, and J. Fontenille, J. Appl. Phys. **51**, 2167 (1980).
[4]Y. Catherine and G. Turban, Thin Solid Films **70**, 101 (1980).
[5]D. Engemann, R. Fischer, and J. Knecht, Appl. Phys. Lett. **32**, 567 (1978).
[6]R. S. Sussmann and R. Ogden, Philos. Mag. B **44**, 137 (1981).
[7]Y. Catherine, G. Turban, and B. Grolleau, Thin Solid Films **76**, 23 (1981).
[8]Y. Tawada, H. Okamoto, and Y. Hamakawa, Appl. Phys. Lett. **39**, 237 (1981).
[9]Y. Tawada, M. Kondo, H. Okamoto, and Y. Hamakawa, in Proceedings of the Ninth International Conference on Amorphous and Liquid Semiconductors, Grenoble, published as J. Phys. Paris Colloq. **4**, 471 (1981).
[10]H. Munekata, S. Murasato, and H. Kukimoto, Appl. Phys. Lett. **37**, 536 (1980).
[11]Y. Tawada, T. Yamaguchi, S. Nonomura, S. Hotta, H. Okamoto, and Y. Hamakawa, Jpn. J. Appl. Phys. **20**, Suppl. 20-2, 219 (1981).
[12]Y. Tawada, M. Kondo, H. Okamoto, and Y. Hamakawa, in *Proceedings of the 15th IEEE Photovoltaic Specialists Conference*, Florida (IEEE, New York, 1981), p. 245.
[13]Y. Tawada, M. Kondo, H. Okamoto, and Y. Hamakawa, in *Proceedings of the 13th Conference on Solid-State Devices* (Tokyo, 1981); published as Jpn. J. Appl. Phys. **21**, Suppl. 21-1, 297 (1982).
[14]E. A. Davis and N. F. Mott, Philos. Mag. **22**, 903 (1970).
[15]P. J. Zanzzuchi, C. R. Wronski, and D. E. Carlson, J. Appl. Phys. **48**, 5227 (1977).
[16]K. M. Mackay and R. Watt, Spectrochim. Acta A **23**, 2761 (1967).
[17]Y. Katayama and T. Shimada, Jpn. J. Appl. Phys. **19**, Suppl. 19-2, 115 (1980).
[18]M. H. Brodsky, M. Cardona, and J. J. Cuomo, Phys. Rev. B **16**, 3556 (1977).
[19]C. C. Tsai and H. Fritzsche, Sol. Energy **1**, 29 (1979).
[20]G. Lucovsky, Solid State Commun. **29**, 571 (1979).
[21]C. J. Fang, K. J. Gruntz, L. Ley, and M. Cardona, J. Non Cryst. Solids **35/36**, 255 (1980).
[22]H. Okamoto, Y. Nitta, T. Yamaguchi, and Y. Hamakawa, Sol. Energy **2**, 313 (1980).
[23]Y. Tawada, M. Kondo, H. Okamoto, and Y. Hamakawa, Sol. Energy (to be published).